ELSEVIER

Journal of Molecular Catalysis A: Chemical 150 (1999) 251–266

JOURNAL OF MOLECULAR CATALYSIS A: CHEMICAL

www.elsevier.com/locate/molcata

Characterization and catalytic activity of iron(III) mono(4-*N*-methyl pyridyl)-tris(halophenyl) porphyrins in homogeneous and heterogeneous systems

Cynthia M.C. Prado-Manso [a], Ednalva A. Vidoto [b], Fábio S. Vinhado [a], Hérica C. Sacco [a,c], Katia J. Ciuffi [a,d], Patrícia R. Martins [a], Antônio G. Ferreira [e], John R. Lindsay-Smith [f], Otaciro R. Nascimento [b], Yassuko Iamamoto [a,*]

[a] *Departamento de Química, FFCLRP, Universidade de São Paulo, Av. Bandeirantes, 3900, CEP 14040-901, Ribeirão Preto, SP, Brazil*
[b] *Instituto de Física de São Carlos, USP, São Carlos, SP, Brazil*
[c] *Instituto de Química, UNESP, Araraquara, SP, Brazil*
[d] *Departamento de Química, Universidade de Franca, Franca, SP, Brazil*
[e] *Departamento de Química, UFSCar, São Carlos, SP, Brazil*
[f] *Department of Chemistry, University of York, York, YO10 5DD, UK*

Received 10 December 1998; accepted 7 April 1999

Abstract

The synthesis, characterization and catalytic activity of the cationic iron porphyrins Fe[M(4-*N*-MePy)TDCPP]Cl_2 and Fe[M(4-*N*-MePy)TFPP]Cl_2 in the epoxidation of (*Z*)-cyclooctene by PhIO in homogeneous solution and supported on silica gel (SG), imidazole propyl gel (IPG) or SG modified with 2-(4-sulfonatophenyl)ethyl groups ($SiSO_3$) have been accomplished. When supported on IPG, both cationic FeP bind to the support via Fe–imidazole coordination. Fe[M(4-*N*-MePy)TDCPP]IPG contains a mixture of low-spin bis-coordinated $Fe^{III}P$ and high-spin mono-coordinated $Fe^{III}P$ species, whereas Fe[M(4-*N*-MePy)TFPP]IPG only contains high-spin mono-coordinated $Fe^{III}P$. These FePIPG catalysts also contain $Fe^{II}P$ species, whose presence was confirmed by EPR spectroscopy using NO as a paramagnetic probe. Both cationic FePs coordinate to SG through Fe–O ligation and they are present as high-spin $Fe^{III}P$ species. The cationic FePs supported on $SiSO_3^-$ are also high-spin $Fe^{III}P$ species and they bind to the support via electrostatic interaction between the 4-*N*-methyl-pyridyl groups and the SO_3^- groups present on the matrix. In homogeneous solution, both Fe[M(4-*N*-MePy)TDCPP]Cl_2 and Fe[M(4-*N*-MePy)TFPP]Cl_2 have similar catalytic activity to Fe(TDCPP)Cl and Fe(TFPP)Cl, leading to *cis*-epoxycyclooctane yields of 92%. When supported on inorganic matrices, both FePs lead to epoxide yields comparable to their homogeneous analogues and their anchoring enables catalyst recovery and re-use. Recycling of Fe[M(4-*N*-MePy)TDCPP]$SiSO_3^-$ shows that this FeP maintains its activity in a second reaction. © 1999 Elsevier Science B.V. All rights reserved.

Keywords: Cationic iron(III) porphyrin; Porphyrin; (*Z*)-Cyclooctene epoxidation; Supported catalysts; Anionic matrix

* Corresponding author. Tel.: +55-16-6023716; fax: +55-16-6338151; e-mail: iamamoto@usp.br

1381-1169/99/$ - see front matter © 1999 Elsevier Science B.V. All rights reserved.
PII: S1381-1169(99)00216-2

1. Introduction

The development of efficient catalytic systems for oxidation reactions that mimic the action of cytochrome *P*-450-dependent monooxygenases has attracted much interest in recent years [1–6]. Synthetic metalloporphyrins have been used as cytochrome *P*-450 models to catalyze the transfer of an oxygen atom from a great variety of oxidizing agents into hydrocarbon molecules. The first system described by Groves et al. [7] which used Fe(TPP)Cl (Fig. 1) and iodosylbenzene (PhIO) in the oxidation of cyclohexane was able to mimic the reactions of the short catalytic cycle of cytochrome *P*-450. The main drawback for practical use of this protein-free FeP system was the oxidative self-destruction of the catalyst. One way to circumvent this problem has been to create more resistant porphyrin ligands through the introduction of electron-withdrawing substituents on the *meso*aryl and/or β-pyrrole positions of the tetraphenylporphyrin (Fig. 1) [5,8–10].

The stability of metalloporphyrin catalysts may also be improved by binding them to solid surfaces. This can provide added benefits aris-

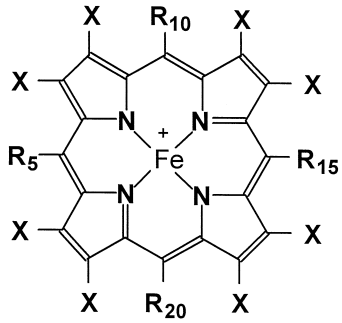

R_5=R_{10}=R_{15}=R_{20}=	X=	FeP
Phenyl	H	$Fe(TPP)^+$
Pentafluorophenyl	H	$Fe(TFPP)^+$
2,6-dichlorophenyl	H	$Fe(TDCPP)^+$
2,6-dichlorophenyl	Cl	$Fe(TDCPCl_8P)^+$
pentafluorophenyl	Cl	$Fe(TFPCl_8P)^+$
2-N-methylpyridyl	H	$Fe[T(2\text{-}N\text{-}MePy)P]^{5+}$
4-N-methylpyridyl	H	$Fe[T(4\text{-}N\text{-}MePy)P]^{5+}$
2,6-dichloro-3-sulfonatophenyl	H	$Fe(TDCSPP)(Cl)^{4-}$
3-sulfonatophenyl	H	$Fe(TSPP)(Cl)^{4-}$

R_5=R_{10}=R_{15}=	X=	R_{20}=	FeP
2,6-dichlorophenyl	H	4-N-methylpyridyl	$Fe[M(4\text{-}N\text{-}MePy)TDCPP]^{2+}$
Pentaflurophenyl	H	4-N-methylpyridyl	$Fe[M(4\text{-}N\text{-}MePy)TFPP]^{2+}$

Fig. 1. Iron(III) porphyrins.

ing from steric and electronic effects of the support which are in some respects analogous to the influence of the polypeptide chain in hemoproteins [11]. Supporting metalloporphyrins also provides site-isolation of the metal centre, thus minimizing catalyst self-destruction and dimerization of unhindered metalloporphyrins such as $Fe(TPP)^+$ and $Fe(TFPP)^+$ [12]. Furthermore, in the era of ''clean technology'', heterogeneous catalytic oxidations have become an important target since they have the potential of replacing the traditional stoichiometric processes used in industry, helping to minimize the problems of industrial waste treatment and disposal [5].

Silica gel (SG) is an attractive support for metalloporphyrins since it is oxidatively stable even under extreme conditions [1]. Since the role of iron protoporphyrin IX in biological systems is strongly dependent on the axial ligand to the iron centre, another approach to the design of models for hemoproteins is to use silica as a coordinative support. This requires converting the surface silanol groups into silylpropyl derivatives such as propyl imidazole (IPG, Fig. 2), which act as ligands for the metalloporphyrin [13–15] and play the role of moderating the metal ion's activity [4].

The great majority of studies on the catalytic activity of metalloporphyrins have used apolar catalysts in organic media. The development of ionic metalloporphyrins is very important since it opens the possibility of using such catalysts adsorbed on matrices through electrostatic interactions with the counterionic groups on the surface of the support, as for example, on $SiSO_3^-$ (Fig. 2) [16]. The main advantages of this approach are the strong interactions between the metalloporphyrin and support and the simplicity of the catalyst preparation. In fact, such ionic interactions are generally stronger than the coordinative binding of the metalloporphyrin to the support [17]. Leanord and Lindsay-Smith [18,19] have reported the use of $Fe[T(4\text{-}N\text{-}MePy)P]^{5+}$, $Fe[T(2\text{-}N\text{-}MePy)P]^{5+}$, $Fe(TSPP)^{3-}$ and $Fe(TDCSPP)^{3-}$ supported on ion exchange resins as catalysts in the oxidation of cyclohexene and (*Z*)-cyclooctene. Meunier et al. [20] have reported the use of sulfonated MnPs supported on methylated poly(4-vinylpyridinium) polymers as catalysts for the oxidative degradation of lignin model compounds.

Iamamoto et al. [21–26] have already reported studies on the characterization and catalytic activity of Fe(TPP)Cl, Fe(TDCPP)Cl, Fe(TFPP)Cl, Mn(TPP)Cl, Mn(TDCPP)Cl and Mn(TFPP)Cl in the oxidation of cyclohexane by PhIO, in both homogeneous systems and supported on SG or imidazole propyl gel (IPG). In this work, we have synthesized a new class of cationic FeP bearing electron-withdrawing substituents in the *meso*aryl positions of the porphyrin ring: $Fe[M(4\text{-}N\text{-}MePy)TDCPP]Cl_2$ and $Fe[M(4\text{-}N\text{-}MePy)TFPP]Cl_2$ (Fig. 1). The aim of this work has been to study and compare the catalytic activity of these FePs in the epoxidation of (*Z*)-cyclooctene by PhIO in three different systems: (i) homogeneous systems, (ii) supported on IPG through coordinative binding and (iii) supported on $SiSO_3^-$ through electrostatic interaction (Fig. 2). The FePs supported on the unmodified support SG were also studied for comparison.

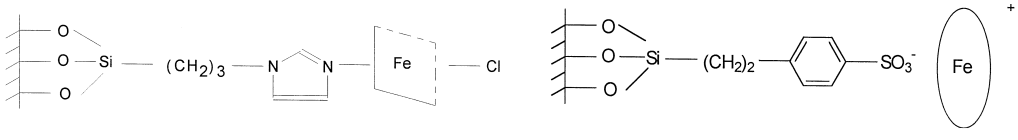

Fig. 2. Iron porphyrin-IPG and cationic iron porphyrin-$SiSO_3^-$.

2. Experimental

2.1. Materials

All solvents and reagents were of commercial grade unless otherwise stated and were purchased from Merck and Aldrich. Pyrrole was distilled under reduced pressure immediately before use. Dichloromethane (DCM) was left over anhydrous $CaCl_2$ for 2.5 h, then filtered and distilled over P_2O_5 and kept over 4 Å molecular sieves. Cyclohexane was distilled over P_2O_5 and kept over 4 Å molecular sieves. Methanol was distilled from magnesium and solid I_2 and kept over 4 Å molecular sieves. Petroleum ether was distilled prior to use. 1,2-dichloroethane (DCE) was distilled and stored over 4 Å molecular sieves. Acetonitrile (ACN) was stored over 3 Å molecular sieves. *N,N*-dimethylformamide (DMF) was stirred over KOH at room temperature overnight, decanted and then distilled at reduced pressure. (*Z*)-Cyclooctene purity was determined by gas chromatographic analysis and it was purified by column chromatography on basic alumina prior to use.

2.1.1. PhIO

This was obtained through the hydrolysis of iodosylbenzenediacetate [27]. Samples were stored in a freezer and the purity was checked every 6 months by iodometric assay.

2.1.2. Iron(III) porphyrins

2.1.2.1. Fe(TDCPP)Cl and Fe(TFPP)Cl. $TDCPPH_2$ and $TFPPH_2$ were purchased from Midcentury and iron insertion into the free-base porphyrins was carried out under argon in DMF, using $FeBr_2 \cdot 2H_2O$ [28]. DMF was removed under vacuum and the products Fe(TDCPP)Br [λ_{max}, nm (DMF) = 392, 418, 508, 570, 642] and Fe(TFPP)Br [λ_{max}, nm (DMF) = 344, 396, 504, 558 nm] were washed with water to remove $FeBr_2 \cdot 2H_2O$ and this process converted the iron porphyrins into Fe(TDCPP)OH [λ_{max}, nm (DCM) = 334, 414, 574] and $[Fe(TFPP)]_2O$ [λ_{max}, nm (DCM) = 326, 398, 560], which were purified by silica column chromatography using a gradient mixture of 5%–10% methanol in DCM or cyclohexane/DCM 2:3 mixture as eluents, respectively. The unreacted free-base porphyrins were eluted first, followed by Fe(TDCPP)OH or $[Fe(TFPP)]_2O$. The DCM solutions of Fe(TDCPP)OH and $[Fe(TFPP)]_2O$ were treated with HCl gas, which converted them into Fe(TDCPP)Cl and Fe(TFPP)Cl. These FePs were isolated by removing the solvent DCM under vacuum. Fe(TDCPP)Cl. UV-Vis (DCM) λ_{max}, nm (ε, mol^{-1} l cm^{-1}) 375, 416 (9.4×10^4, Soret band), 506 (1.1×10^4), 578, 644. Fe(TFPP)Cl. UV-Vis (DCM) λ_{max}, nm (ε, mol^{-1} l cm^{-1}) 352, 412 (1.8×10^5, Soret band) 504 (1.7×10^4), 576, 630.

2.1.2.2. Fe[M(4-N-MePy)TDCPP]Cl_2 and Fe[M(4-N-MePy)TFPP]Cl_2. The syntheses of the 4-*N*-methylpyridyl-substituted free-base porphyrins were carried out by the method described by Adler et al. [29,30], through the co-condensation of pyrrole, 4-pyridinecarboxyaldehyde and 2,6-dichlorobenzaldehyde or pentafluorobenzaldehyde in a 5 or 4:1:4 molar ratio, respectively, in glacial acetic acid, at 150°C. The crude product was initially purified by column chromatography on florisil, using a solvent mixture dichloromethane/petroleum ether 3:1 as eluent. In the case where 2,6-dichlorobenzaldehyde was used, four spots were detected through TLC analysis of the product. When pentafluorophenylbenzaldehyde was used, two spots were detected. The 2,6-dichlorophenyl-substituted and the pentafluorophenyl-substituted porphyrins were separated by column chromatography on silica using a gradient mixture of 0%–5% methanol in DCM in the former case and a cyclohexane/DCM 2:1 solvent mixture followed by 8% acetone in DCM, in the latter case. The purified products were identified as being $TDCPPH_2$, M(4-*N*-Py)TDC-PPH_2, *cis*-B(4-*N*-Py)BDCPPH_2, T(4-*N*-Py)MD-CPPH_2, $TFPPH_2$ and M(4-*N*-Py)TFPPH_2 by ^1H NMR and FAB MS analyses. The H_2Ps

yields based on pyrrole were: 0.8%, 1.0%, 0.8%, 1.4% and 8.6%, respectively.

M(4-*N*-Py)TDCPPH$_2$ and M(4-*N*-Py)TFPPH$_2$ were methylated by reaction with excess CH_3I in DMF at room temperature, under argon [31]. After removal of the unreacted CH_3I and DMF under vacuum, the methylated porphyrins were dissolved in methanol and precipitated with diethyl ether. The iodide anion was exchanged for chloride using a Dowex 1 X 2-200 1-chloride ion exchange resin.

Iron insertion into M(4-*N*-MePy)TDCPPH$_2$Cl and M(4-*N*-MePy)TFPPH$_2$Cl was achieved by heating the free-base porphyrins and $FeCl_2 \cdot 4H_2O$ at reflux in acetonitrile for 3 h [32]. At the end of the reaction, acetonitrile was removed under vacuum. The FeP were dissolved in water and $NaClO_4$ was added to the solution, producing a dark precipitate. The mixture was chilled overnight and the solid FeP were isolated by filtration. The perchlorate anion was exchanged with chloride using an ion exchange resin.

2.1.2.3. M(4-N-Py)TFPPH$_2$. UV-Vis (DCM) λ_{max}, nm (ε, mol^{-1} l cm^{-1}) 412 (3.1×10^5, Soret band), 506, 536 (shoulder), 582, 636 (weak). ^{1}H NMR ($CDCl_3$) $\delta = 9.07$ (dd, $J =$ 1.51 and 4.14 Hz, 2H 3,5-pyridyl), $\delta = 8.93$ (s, 4H β-pyrrole), $\delta = 8.92$ (d, $J = 4.89$ Hz, 2H β-pyrrole), $\delta = 8.87$ (d, $J = 4.89$ Hz, 2H β-pyrrole), $\delta = 8.17$ (dd, $J = 1.51$ and 4.14 Hz, 2H 2,6-pyridyl), $\delta = -2.58$ (s, 2H N–H pyrrole), FAB MS [M] = 886. R_f silica/15% MeOH in DCM = 0.81.

2.1.2.4. M(4-N-Py)TDCPPH$_2$. UV-Vis (DCM) λ_{max}, nm (ε, mol^{-1} l cm^{-1}) 418 (2.5×10^5, Soret band), 512 (1.4×10^4), 588 (7.8×10^3). ^{1}H NMR ($CDCl_3$) $\delta = 9.01$ (d, $J = 5.00$ Hz, 2H 3,5-pyridyl), $\delta = 8.77$ (d, $J = 5.0$ Hz, 2H β-pyrrole), $\delta = 8.69$ (d, $J = 5.0$ Hz, 2H β-pyrrole), $\delta = 8.67$ (s, 4H β-pyrrole), $\delta = 8.16$ (d, $J = 5.00$ Hz, 2H 2,6-pyridyl), $\delta = 7.80$ (q AB_2, $J = 8.21$ Hz, 4H 3,5-dichlorophenyl), $\delta = 7.79$ (q AB_2, $J = 8.21$ Hz, 2H 3,5-dichlorophenyl), $\delta = 7.70$ (q AB_2, $J = 8.21$ Hz, 2H 4-dichlorophenyl), $\delta = 7.69$ (q AB_2, $J = 8.21$ Hz, 1H 4-dichlorophenyl), $\delta = -2.58$ (s, 2H N–H pyrrole), FAB MS [M] = 822. R_f silica/8% MeOH in DCM = 0.95.

2.1.2.5. M(4-N-MePy)TFPPH$_2$Cl. UV-Vis (DCM) λ_{max}, nm (ε, mol^{-1} l cm^{-1}) 418 (3.0×10^4, Soret band), 506, 538 (shoulder), 582. ^{1}H NMR ($CDCl_3$) $\delta = 9.72$ (dd, 2H, 3,5-pyridyl), $\delta = 9.08$ (dd, 2H, 2,6-pyridyl), $\delta = 8.97$ (d, 2H β-pyrrole), $\delta = 8.92$ (s, 4H β-pyrrole), 8.78 (d, 2H β-pyrrole), $\delta = 5.07$ (s, 3H, N^+-methyl), $\delta = -2.98$ (s, 2H, pyrrole), R_f silica/15% MeOH in DCM = 0.60.

2.1.2.6. M(4-N-MePy)TDCPPH$_2$Cl. UV-Vis (MeOH) λ_{max}, nm (ε, mol^{-1} l cm^{-1}) 416 (3.3×10^4, Soret band), 512 (3.3×10^3), 548 (1.4×10^3), 588 (7.8×10^3), 658 (7.5×10^3). ^{1}H NMR ($CDCl_3$) $\delta = 8.9$ a 9.1 (m, 2H, 3,5-pyridyl), $\delta = 8.6$ a 8.8 (m, 8H β-pyrrole), $\delta =$ 8.2 a 8.4 (m, 2H, 2,6-pyridyl), $\delta = 7.6$ a 7.9 (m, 9H 3,5-dichlorophenyl and 4-dichlorophenyl), $\delta = 4.6$ (s, 3H, N^+-methyl), $\delta = -2.6$ (s, 2H, pyrrole), ES MS 836 $[M-Cl^-]^+$. R_f silica/8% MeOH in DCM = 0.18.

2.1.2.7. Fe[M(4-N-MePy)TFPP]Cl$_2$. UV-Vis (DCE) λ_{max}, nm (ε, mol^{-1} l cm^{-1})360, 418 (2.9×10^4, Soret band), 504, 580, 640. ES MS 989 $[M-Cl^-]^+$, 954 $[M-2Cl^-]^+$. R_f silica/15% MeOH in DCM = 0.28.

2.1.2.8. Fe[M(4-N-MePy)TDCPP]Cl$_2$. UV-Vis (DCE) λ_{max}, nm (ε, mol^{-1} l cm^{-1}362, 420 (1.6×10^4, Soret band), 508, 640, ES MS 890 $[M-2Cl^-]^+$, R_f silica/8% MeOH in DCM = 0.16.

2.1.3. Solid supports

SG was dried by heating at 60°C (5 mmHg) for 4 h. IPG and $SiSO_3^-$ were prepared by the method described by Leal et al. [13]. IPG Elemental analysis: C = 5.24, H = 1.22, N = 0.26, which corresponds to 9.3×10^{-5} mol of imida-

zole per gram of IPG. $SiSO_3^-$ Elemental analysis: C = 5.41, H = 0.94, which corresponds to 5.5×10^{-4} mol of SO_3^- per gram of $SiSO_3^-$.

2.1.4. Preparation of supported metalloporphyrins

FeP ligation to the solid supports was achieved by stirring a DCM solution of FeP with a suspension of the support for 10–20 min. The resulting supported catalyst was washed with DCE (the solvent to be used in the epoxidation reactions) in a Soxhlet extractor overnight to remove unbound and weakly bound porphyrin. The solid catalyst was isolated by filtration and was then dried for 3 h at 80°C. The loadings were quantified by measuring the amount of unloaded FeP, in the combined reaction solvent and washings, by UV-Vis spectroscopy.

2.2. UV-Vis spectra

The UV-Vis spectra were recorded on a Hewlett-Packard 8452 Diode Array UV-Vis spectrophotometer. In the case of supported FeP, spectra were recorded in a 2 mm path length quartz cell, using a suspension of a mixture of the supported catalyst and the support itself in CCl_4. The ''blank'' was recorded previously and consisted of a support/CCl_4 suspension.

2.3. EPR spectra

The EPR spectra were recorded on a Varian E-109 century line spectrometer operating at the X-band, at a temperature of ca. 4 K. The *g* values were calculated by taking the frequency indicated in a HP 5340 A frequency meter and the field measured at the spectral features, which were recorded with increased gain and expanded field. Routine calibrations of the field setting and scan were made with DPPH and Cr^{3+} reference signals. The Helitran (Oxford Systems) low temperature accessory was employed to obtain the spectra in the specified temperature range.

2.3.1. EPR spectra of supported FeP

The EPR spectra of supported FeP were recorded at a temperature of ca. 4 K after addition of 0.0400–0.0700 g of the supported catalyst to an EPR tube containing 200 μl DCE.

2.3.2. Addition of NO to FePIPG

The EPR tube containing ~0.0650 g of FePIPG was deaerated with N_2 for 1 h. Afterwards, N_2 was removed under vacuum and 2 ml NO (generated from the reaction between Cu^o and HNO_3 in a special apparatus) were added to the catalyst and the EPR spectrum was obtained at a temperature of ca. 4 K.

2.4. ^{1}H NMR spectra

^{1}H NMR spectra were accomplished on a Brüker DR XC 400, 9.4 T spectrometer using TMS as internal reference.

2.5. ES MS spectra

Electrospray mass spectra were recorded on an LCQ Finnigon MAT spectrometer.

2.6. Epoxidation reactions

Controls for all reactions were carried out in the absence of FeP.

2.6.1. Homogeneous catalysis

The reactions were carried out in a 2 ml vial sealed with a teflon-coated silicone septum. A total of 400 μl FeP solution in DCE (6.0×10^{-4} mol l^{-1}), 400 μl (*Z*)-cyclooctene and 100 μl cyclohexanone solution in DCE (6.0×10^{-2} mol l^{-1}; internal standard) were added to the vial containing PhIO (~5.00 mg) under argon. The mixture was protected from light and stirred at room temperature, for the desired time and the build-up of *cis*-epoxycyclooctane was moni-

tored by removing 3 μl aliquots of the reaction mixture for analysis by gas chromatography.

2.6.2. Heterogeneous catalysis

The reactions were carried out in an 8 ml vial sealed with a teflon-coated silicone septum. A total of 1600 μl DCE, 1600 μl (*Z*)-cyclooctene and 100 μl cyclohexanone solution in DCE (6.0×10^{-2} mol l^{-1}; internal standard) were added to the vial containing PhIO (~ 5.00 mg) and the supported FeP (50 mg) under argon. The mixture was protected from light and stirred at room temperature, for the desired time. The reaction was monitored as described above.

2.6.3. Re-use of the catalyst Fe[M(4-N-MePy)TDCPP]$SiSO_3^-$

At the end of the reaction, the catalyst Fe[M(4-*N*-MePy)TDCPP]$SiSO_3^-$ was recovered by centrifugation and washed five times with 1 ml DCE to ensure that any remaining PhIO was removed from the catalyst. The catalyst was then dried for 3 h at 60°C, before being used again in an oxidation reaction.

2.6.4. Product analysis

The products were analyzed by gas chromatography using cyclohexanone as the internal standard. The yields are based on PhIO. Gas chromatographic analyses were performed on either a CG 37-002 gas chromatograph or a CG 500 gas chromatograph coupled to a CG 300 integrator. Nitrogen was used as the carrier gas with an hydrogen flame ionization detector. The inox column (length, 1.8 m; internal diameter, 3 mm) was packed with 10% Carbowax 20M on Chromosorb WHP.

3. Results and discussion

3.1. Epoxidation of (Z)-cyclooctene by PhIO catalyzed by FeP in homogeneous systems

For the initial studies on the catalytic activity of the cationic iron porphyrins: Fe[M(4-*N*-MePy)TFPP]Cl_2 and Fe[M(4-*N*-MePy)-TDCPP]Cl_2, the epoxidation of (*Z*)-cyclooctene by PhIO was selected to compare the efficiency of the supported FeP catalysts with each other and with analogous homogeneous systems. This substrate was chosen for three reasons: (i) it gives a clean conversion into *cis*-epoxycyclooctane without contamination from other alkene oxidation products; (ii) it is easily oxidized, thus preventing loss of the active catalytic intermediate through competitive reactions with PhIO and the FeP itself (see Fig. 3); and (iii) it has been extensively used in earlier metalloporphyrin-catalyzed oxidation reactions [15,16]. PhIO was chosen as oxygen source since (i) it can give good oxidant conversions; (ii) it is relatively inert in the absence of FeP; and (iii) it reacts with FeP generating the $Fe^{IV}(O)P^{\cdot+}$ active catalytic species and PhI [15,17].

All the reactions were carried out in DCE, since this was the best solvent for cyclohexane hydroxylation reactions catalyzed by the apolar Fe(TDCPP)Cl and Fe(TFPP)Cl [22,23], being inert to the active species $Fe^{IV}(O)P^{\cdot+}$, unlike DCM, methanol or acetonitrile [22,23]. Table 1 and Fig. 4 show the results obtained with Fe[M(4-*N*-MePy)TFPP]Cl_2 and Fe[M(4-*N*-MePy)TDCPP]Cl_2 and the results for Fe(TDCPP)Cl and Fe(TFPP)Cl are also included for comparison. The catalytic activities of Fe[M(4-*N*-MePy)TDCPP]Cl_2 and Fe[M(4-*N*-MePy)-TFPP]Cl_2 are very comparable to those of the corresponding apolar Fe(TDCPP)Cl and

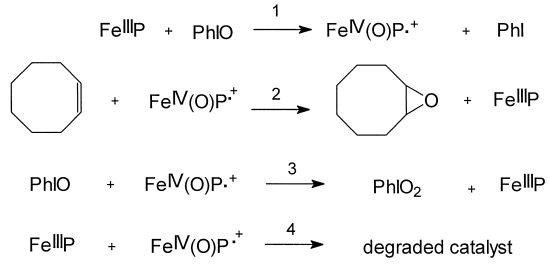

Fig. 3. Mechanism for the hydroxylation of (*Z*)-cyclooctene by PhIO and iron(III)porphyrin and possible competitive reactions [33].

Table 1
Catalytic activity of FeP in the epoxidation of (*Z*)-cyclooctene by PhIO in homogeneous systems
Reaction conditions: argon atmosphere, $T = 25°C$, magnetic stirring, solvent: DCE, (*Z*)-cyclooctene/PhIO/FeP molar ratio = 1.2×10^4:100:1, [FeP] = 3.0×10^{-4} mol l^{-1}.

FeP	Cox (%)[a]	Reaction time (min)	FeP recovery
–[b]	5	60	–
Fe(TDCPP)Cl	92	90	100
Fe[M(4-*N*-MePy)-TDCPP]Cl_2	92	30	90
Fe(TFPP)Cl	80	60	100
Fe[M(4-*N*-MePy)-TFPP]Cl_2	92	120	100

[a] *Cis*-epoxycyclooctane yield (Cox) based on PhIO.
[b] [PhIO] = 5.7×10^{-3} mol l^{-1}.

Fe(TFPP)Cl for the epoxidation of (*Z*)-cyclooctene by PhIO (*cis*-epoxycyclooctane yield ~ 80%–90%). The yield of PhI in all the reactions was 100%, showing that all the oxidant was converted to PhI and the competitive reaction 3 (Fig. 3) between PhIO and the active catalytic species $Fe^{IV}(O)P^{\cdot+}$ does not occur [33].

Examination of FeP through UV-Vis spectroscopy at the end of these reactions shows effectively 100% recovery for Fe(TDCPP)Cl and Fe[M(4-*N*-MePY)TFPP]Cl_2, whereas the recovery of Fe[M(4-*N*-MePy)TDCPP]Cl_2 is consistently ca. 90%. In the case of the latter FeP, some catalyst self-destruction (reaction 4, Fig. 3) may be occurring.

The build-up of *cis*-epoxycyclooctane with time in the (*Z*)-cyclooctene epoxidation (Fig. 4) shows that Fe[M(4-*N*-MePy)TDCPP]Cl_2 is the most active catalyst, being better than its apolar analogue Fe(TDCPP)Cl. This is probably because the former FeP confers less steric hindrance to the approach of (*Z*)-cyclooctene to the active catalytic species $Fe^{IV}(O)P^{\cdot+}$, since it contains less chloro-substituents than Fe(TDCPP)Cl. The reactions of Fe[M(4-*N*-MePy)TFPP]Cl_2 take longer than those of Fe(TDCPP)Cl and Fe[M(4-*N*-MePy)TDCPP]Cl_2 to reach the maximum epoxide yield (Fig. 4). It is likely that this is because the fluoro-substituted iron porphyrin is relatively unhindered and can aggregate through $\pi-\pi$ interactions (Fig. 5) [34], resulting in a less active catalyst than the monomer. Such aggregation is confirmed by the fact that this FeP does not obey Beer's law in concentrations above 5.0×10^{-5} mol l^{-1}. So, in the case of Fe[M(4-*N*-MePy)TFPP]Cl_2, the substrate accessibility to the active site of the FeP may be hampered by the aggregation process, which accounts for the lower reaction rate.

3.2. Preparation of supported FeP catalysts

SG surface modification with imidazole-propyl groups, to give the support IPG (Fig. 2) and with 2-(4-sulfonatophenyl)ethyl groups, to give the support $SiSO_3^-$ (Fig. 2) was carried out through the method described by Leal et al. [13]. If it is assumed that there are 4.2×10^{-3} mol silanol groups per gram of SG [15,17] and that the SG surface modification to give either IPG or $SiSO_3^-$ involves three silanol groups [13], the elemental analyses show the loading of imidazole and 4-sulfonatophenyl to involve 7% and 40% of the surface silanol groups for IPG and $SiSO_3^-$, respectively.

The supported FeP were prepared by stirring a suspension of the support (SG, IPG and $SiSO_3^-$) in a solution of FeP in DCM. These materials were subsequently washed in a Soxh-

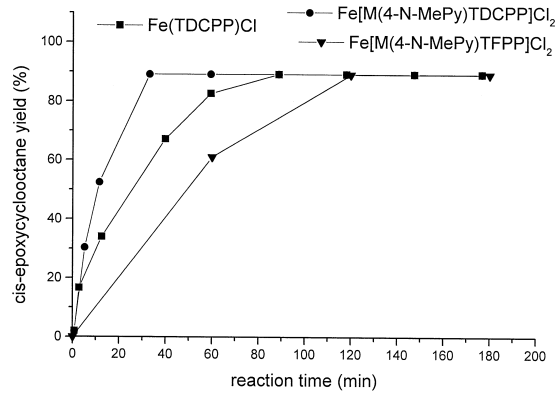

Fig. 4. Time-dependent build-up of *cis*-epoxycyclooctene in the epoxidation of (*Z*)-cyclootene by PhIO catalysed by various FeP in homogenous solution.

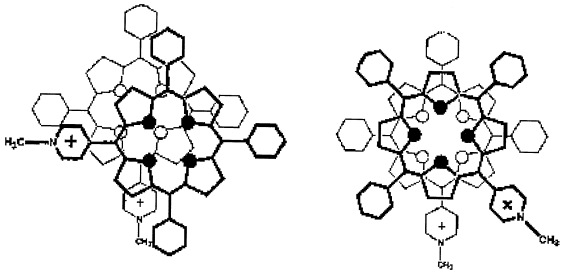

Fig. 5. Possible structure for the self-aggregation of Fe[M(4-*N*-MePy)TFPP]Cl_2 through $\pi-\pi$ interation.

let extractor with DCE overnight, to remove unbound and weakly bound FeP. This ensures that the FeP is not leached from the support throughout the epoxidation reactions that are carried out in DCE at 25°C and that the yields attained with the heterogeneous catalysts are only due to the catalytic activity of supported FeP. The washed catalysts were isolated by filtration and dried for 3 h at 80°C.

$SiSO_3^-$ and IPG were selected as supports because they are oxidatively stable under the reaction conditions and allow the study of the catalytic activity of cationic FeP anchored to solid surfaces by: (i) electrostatic interaction between the 4-*N*-methylpyridyl groups and counterionic groups on the surface of $SiSO_3^-$ and (ii) through coordinating groups on the surface of IPG. Another reason for using $SiSO_3^-$ was that it was expected to give rise to stronger FeP-support binding than IPG [15,17]. The catalytic activities of cationic FeP were also studied when supported on unmodified SG for comparison. Results for $Fe(TDCPP)^+$ and $Fe(TFPP)^+$ supported on both SG and IPG are also presented for comparison.

3.3. Characterization of Fe[M(4-N-MePy)TDCPP]IPG and Fe[M(4-N-MePy)TFPP]IPG through UV-Vis and EPR spectroscopy

To help characterize Fe[M(4-*N*-MePy)-TDCPP]IPG and Fe[M(4-*N*-MePy)TFPP]IPG, solution models were investigated by following the titration of FeP solutions in DCE with aliquots of an imidazole solution also in this solvent.

The UV-Vis spectra of Fe[M(4-*N*-MePy)-TDCPP]Cl_2 and Fe[M(4-*N*-MePy)TFPP]Cl_2 in DCE (Fig. 6A and D, respectively) have absorption bands at $\lambda = 356$, 422 (Soret), 508, 566 and 640 nm and at $\lambda = 360$, 418 (Soret), 504, 580 and 640 nm, respectively. The three peaks present in the region of 500–700 nm are typical of high-spin Fe^{III} porphyrins [35] and the band at $\lambda \sim 360$ nm is typical of FeP–Cl coordina-

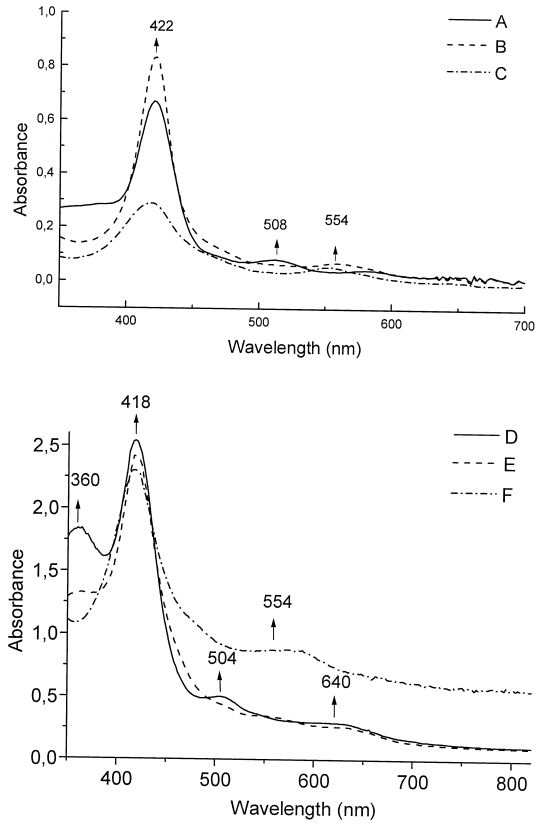

Fig. 6. UV-Vis spectra of: (A) 2.3×10^{-7} mol Fe[M(4-*N*-MePy)TDCPP]Cl_2 in DCE; (B) A after the addition of 1.5×10^{-6} mol imidazole, Im/FeP molar ratio = 6.4; (C) 0.0350 g washed Fe[M(4-*N*-MePy)TDCPP]IPG containing 4.4×10^{-6} mol FeP/g IPG ''diluted'' with 0.0850 g IPG corresponding to 1.5×10^{-7} mol FeP, in CCl_4; (D) 2.5×10^{-7} mol Fe[M(4-*N*-MePy)TFPP]Cl_2 in DCE; (E) A after the addition of 1.0×10^{-6} mol imidazole, Im/FeP molar ratio = 3.9; (F) 0.0350 g washed Fe[M(4-*N*-MePy)TDCPP]IPG containing 4.7×10^{-6} mol FeP/g IPG ''diluted'' with 0.0850 g IPG corresponding to 1.6×10^{-7} mol FeP, in CCl_4; (A, B, D, E: 1 cm; and C, F: 0.2 cm path length cell).

tion [36]. That the two FeP are high-spin Fe^{III} complexes was confirmed by EPR spectroscopy in DCE. Both FeP display similar EPR spectra with high-spin Fe^{III} signals in $g_{\perp} = 5.985$ and $g_{\parallel} = 1.996$ (Fig. 7A).

Upon addition of excess imidazole to the FeP (Im/FeP molar ratio ~ 4), the three bands between 500–700 nm in the UV-Vis spectra of the two $FePCl_2$ are replaced by a single absorption band at $\lambda = 554$ nm (Fig. 6B and E). It is well documented that the addition of nitrogen bases to a solution of $Fe^{III}P$ leads to the formation of $Fe^{III}P$–imidazole complexes with a single absorption band at $\lambda = 550$ nm [35]. Using the method described by Fleischer and Fine [37], the number of imidazole molecules that coordinated to the FeP (n) and the thermodynamic stability constant (β_n) for the complexes obtained at the end of the titration of Fe[M(4-*N*-MePy)TDCPP]Cl_2 and Fe[M(4-*N*-MePy)TFPP]Cl_2 with imidazole are $n = 2$ for both FeP and $\beta_2 = 3.8 \times 10^7$ and 1.3×10^7 mol^{-2} l^2, respectively, confirming that these FeP form stable bis-imidazole complexes. That the bis-imidazole complexes of the two FeP are low-spin was confirmed through EPR studies. The EPR spectra of bis-imidazole-Fe[M(4-*N*-MePy)TDCPP] and bis-imidazole-Fe[M(4-*N*-MePy)TFPP] are very similar and they both display low-spin Fe^{III} signals in $g_z = 2.54$, $g_y = 2.15$ and $g_x = 1.90$ (Fig. 7B).

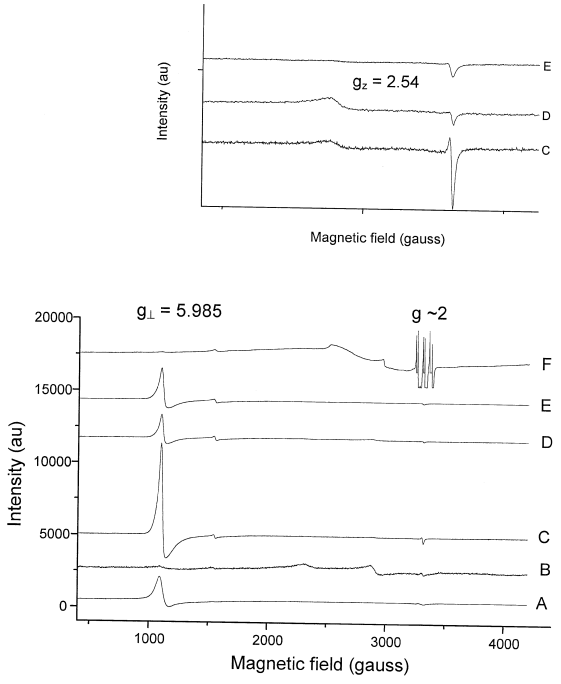

Fig. 7. EPR spectra in DCE (A) Fe[M(4-*N*-MePy)TDCPP]Cl_2 in (100 μl, 9.8×10^{-4} mol l^{-1}), (B) A after the addition of 1.9×10^{-7} mol imidazole; (C) 0.0597 g washed Fe[M(4-*N*-MePy)TDCPP]IPG containing 4.4×10^{-6} mol FeP/g IPG; (D) 0.0604 g unwashed Fe[M(4-*N*-MePy)TDCPP]IPG containing 6.3×10^{-6} mol FeP/g IPG; (E) 0.0597 g washed Fe[M(4-*N*-MePy)TFPP]IPG containing 4.7×10^{-6} mol FeP/g IPG (F) (C) after the addition of 2 ml NO. EPR spectrometer conditions: $T = 4.5$–5.5 K, microwave frequency 9.240 GHz; gain = 2.0×10^3.

By recording the UV-Vis spectra of Fe[M(4-*N*-MePy)TDCPP]IPG (Fig. 6C) and Fe[M(4-*N*-MePy)TFPP]IPG (Fig. 6F), it can be seen that both catalysts display an absorbance band at $\lambda = 554$ nm and Soret bands at $\lambda = 422$ and 416 nm, respectively. Such spectra are very similar to those of the parent FeP–imidazole complexes. The EPR spectrum of Fe[M(4-*N*-MePy)TDCPP]IPG (Fig. 7C) displays high-spin Fe^{III} signals in $g_{\perp} = 5.985$ and $g_{\parallel} = 1.996$ and very weak low-spin Fe^{III} signals in $g_z = 2.54$, $g_y = 2.15$ (g_x not determined) (Fig. 7C, insert). This suggests that most of this FeP is mono-coordinated to the support IPG and that only a small proportion is bis-coordinated to the support. The EPR spectrum of Fe[M(4-*N*-MePy)TFPP]IPG (Fig. 7E and insert) shows only high-spin Fe^{III} signals in $g_{\perp} = 5.985$ and $g_{\parallel} = 1.996$, leading to the conclusion that this FeP is only mono-coordinated to the support.

Interestingly, it seems that washing Fe[M(4-*N*-MePy)TDCPP]IPG in the Soxhlet extractor promotes the conversion of bis-imidazole $Fe^{III}P$ species to mono-imidazole $Fe^{III}P$ species. Fig. 7D shows the EPR spectrum of unwashed Fe[M(4-*N*-MePy)TDCPP]IPG, which displays less intense high-spin Fe^{III} signals in $g_{\perp} =$ 5.985 than the washed catalyst (Fig. 7C).

We have already reported [24] that in the case of Fe(TDCPP)IPG, which contains both high-spin $Fe^{III}PIm$ and low-spin $Fe^{III}P(Im)_2$ species, there is also the presence of the FeP in

its reduced form $Fe^{II}P$. This was confirmed by looking at the EPR spectrum of Fe(TDCPP)IPG in the presence of excess NO [24]. In this work, we have also treated the washed catalysts Fe[M(4-*N*-MePy)TDCPP]IPG and Fe[M(4-*N*-MePy)TFPP]IPG with NO. Upon addition of 2 ml NO to the dry FePIPG catalysts, we observed the appearance of signals in $g \sim 2$, typical of $Fe^{II}NO$ species generated from $Fe^{II}P$ coordination to NO [38,39] (Fig. 7F). Furthermore, the Fe^{III} high-spin signal in $g_{\perp} = 5.985$ disappeared due to the coordination of Fe^{III} to NO, which generates the diamagnetic $Fe^{II}NO^{+}$ species [38,39]. These studies lead to the conclusion that Fe[M(4-*N*-MePy)TDCPP]IPG and Fe[M(4-*N*-MePy)TFPP]IPG contain both $Fe^{II}P$ and $Fe^{III}P$ species.

3.4. Characterization of Fe[M(4-N-MePy)TDCPP]SG, Fe[M(4-N-MePy)TDCPP]SiSO$_3^-$, Fe[M(4-N-MePy)TFPP]SG and Fe[M(4-N-MePy)TFPP]SiSO$_3^-$

To help characterize Fe[M(4-*N*-MePy)TDCPP]SG and Fe[M(4-*N*-MePy)TFPP]SG, solution models were investigated by following the titration of FeP solutions in DCE with aliquots of a tetrabutylammonium hydroxide solution in acetonitrile (prepared according to Ref. [40]).

As described above, the UV-Vis spectra of Fe[M(4-*N*-MePy)TDCPP]Cl_2 and Fe[M(4-*N*-MePy)TFPP]Cl_2 in DCE (Fig. 8A and E, respectively) display absorbance bands at $\lambda = 356$, 422 (Soret), 508, 566 and 640 nm and at $\lambda =$ 360, 418 (Soret), 504, 580 and 640 nm, respectively. Both FeP present similar EPR spectra with high-spin Fe^{III} EPR signals in $g_{\perp} = 5.985$ and $g_{\parallel} = 1.996$ (Fig. 9A).

Upon addition of excess OH^- (OH^-/FeP molar ratio ~ 7), the bands at $\lambda \sim 508$ and 640 nm disappear, and the band at $\lambda = 580$ nm becomes more intense (Fig. 8B and F). Based on the studies of Hatano et al. [41] and Kobayashi et al. [42], who attribute the band at $\lambda = 580$ nm present in the spectra of Fe(TPP)OCH_3 and Fe(TMP)OH to axial coordination of the FeP to oxygen, we assign the band at $\lambda = 580$ nm in the present study to the axial coordination of the FeP to the hydroxide anion. Using the method of Fleischer and Fine [37], we obtained $n = 2$ and $\beta_2 = 5.0 \times 10^7$ mol^{-2} l^2 for the complex formed between Fe[M(4-*N*-

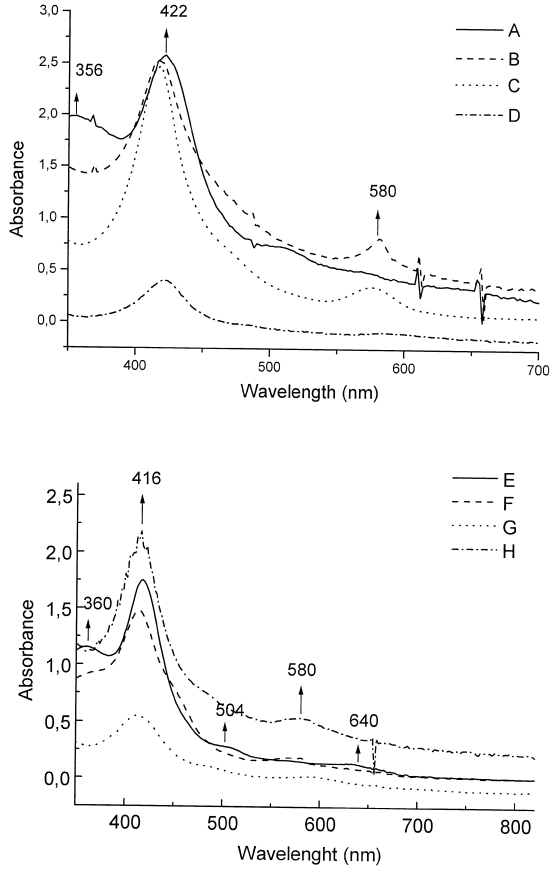

Fig. 8. UV-Vis spectra of (A) 1.0×10^{-7} mol of Fe[M(4-*N*-MePy)TDCPP]Cl_2 in DCE; (B) A after the addition 7.5×10^{-7} mol of TBAOH, OH^-/FeP molar ratio = 7.5; (C) 0.0200 g washed Fe[M(4-*N*-MePy)TDCPP]SG containing 3.6×10^{-6} mol of FeP/g SG ''diluted'' with 0.1800 g SG corresponding to 7.2×10^{-8} mol of FeP, in CCl_4; (D) 0.0250 g washed Fe[M(4-*N*-MePy)TDCPP]$SiSO_3^-$ containing 4.1×10^{-6} mol of FeP/g SG ''diluted'' with 0.0750 g $SiSO_3^-$ corresponding to 1.0×10^{-7} mol FeP, in CCl_4; (E) 1.0×10^{-7} mol Fe[M(4-*N*-MePy)TFPP]Cl_2 in DCE; (F) A after the addition 1.1×10^{-7} mol of TBAOH, OH^-/FeP molar ratio = 1.1; (G) 0.0200 g washed Fe[M(4-*N*-MePy)TFPP]SG containing 4.6×10^{-6} mol FeP/g SG ''diluted'' with 0.1800 g SG corresponding to 9.2×10^{-8} mol FeP, in CCl_4; (H) 0.0250 g washed Fe[M(4-*N*-MePy)TFPP]$SiSO_3^-$ containing 4.8×10^{-6} mol FeP/g SG ''diluted'' with 0.0750 g $SiSO_3^-$ corresponding to 1.2×10^{-7} mol FeP, in CCl_4 (A, B, E, F: 1 cm; and C, D, G, H: 0.2 cm path length cell).

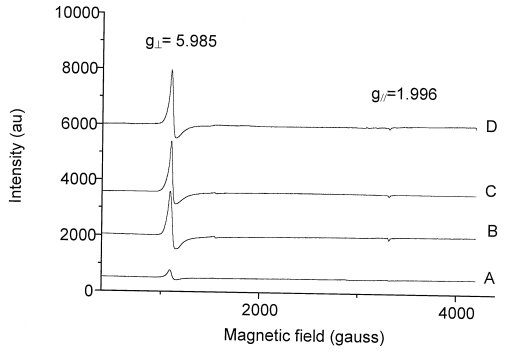

Fig. 9. EPR spectra in DCE of (A) Fe[M(4-*N*-MePy)TDCPP]Cl_2 (100 μl, 8.6×10^{-4} mol l^{-1}); (B) A after the addition of 2.1×10^{-6} mol OH^-; (C) 0.06287 g washed Fe[M(4-*N*-MePy)TDCPP]SG containing 3.6×10^{-6} mol FeP/g SG; (D) 0.0632 g washed Fe[M(4-*N*-MePy)TDCPP]$SiSO_3^-$ containing 4.1×10^{-6} mol FeP/g $SiSO_3^-$. EPR spectrometer conditions: T = 4.5–5.5 K, microwave frequency 9.240 GHz; gain = 1.25×10^3 (A and B); 63 (C); 1.6×10^3 (D).

MePy)TFPP]Cl_2 and OH^-, leading to the conclusion that the stable bis-hydroxide-Fe[M(4-*N*-MePy)TFPP] complex was formed. For Fe[M(4-*N*-MePy)TDCPP]Cl_2, we found $n = 1$ and $K = 4.0\times10^4$ mol^{-1} l, showing that the latter FeP forms a mono-hydroxide complex. The EPR spectra of both FeP in the presence of excess OH^- are very similar and they display high-spin Fe^{III} signals in $g_\perp = 5.985$ and $g_\parallel = 1.996$, showing that both monohydroxide-Fe[M(4-*N*-MePy)TDCPP] and bis-hydroxide-Fe[M(4-*N*-MePy)TFPP] are high-spin Fe^{III} complexes (Fig. 9B).

The UV-Vis spectra of Fe[M(4-*N*-MePy)-TDCPP]SG and Fe[M(4-*N*-MePy)TFPP]SG (Fig. 8C and G, respectively) display absorption bands at $\lambda = 574$ and 584 nm, respectively. As such spectra are very similar to those of the parent FeP–OH^- complexes, there is strong evidence that this band at $\lambda \sim 580$ nm is due to FeP–oxygen coordination. This suggests that the FeP may be coordinated to the silanol groups present on the surface of the support. The EPR spectra of Fe[M(4-*N*-MePy)TDCPP]SG and Fe[M(4-*N*-MePy)TFPP]SG both display high-spin Fe^{III} signals in $g_\perp = 5.985$ and $g_\parallel = 1.996$ (Fig. 9C), as do both FePs when they coordinate to OH^- ions (Fig. 9B), reinforcing the suggestion that the FeP coordinate to the silanol groups on the surface of the support. However, it must be borne in mind that some of the FeP may also be electrostatically bound to SG through electrostatic interaction between the 4-*N*-methylpyridyl group and the support.

The UV-Vis spectra of Fe[M(4-*N*-MePy)TDCPP]$SiSO_3^-$ and Fe[M(4-*N*-MePy)TFPP]$SiSO_3^-$ (Fig. 8D and H, respectively) present typical FeP Soret band at $\lambda = 422$ and 416 nm, respectively. It is thought that in this case, the FeP is anchored to the support through electrostatic interaction between the FeP 4-*N*-methylpyridyl groups and the support $SiSO_3^-$. A fact that reinforces such suggestion is that washing Fe[M(4-*N*-MePy)TDCPP]$SiSO_3^-$ in the Soxhlet extractor removes only 10% of the anchored FeP, while washing Fe[M(4-*N*-MePy)-TDCPP]SG or Fe[M(4-*N*-MePy)TDCPP]IPG removes 30%. So ligation of Fe[M(4-*N*-MePy)TDCPP]$^{2+}$ and Fe[M(4-*N*-MePy)TFPP]$^{2+}$ to $SiSO_3^-$ occurs through electrostatic interaction, which is stronger than FeP interaction with SG or IPG. The EPR spectra of both Fe[M(4-*N*-MePy)TDCPP]$SiSO_3^-$ and Fe[M(4-*N*-MePy)TFPP]$SiSO_3^-$ display signals in $g_\perp = 5.985$ and $g_\parallel = 1.996$ (Fig. 9D), which show that these catalysts contain high-spin Fe^{III} species.

Unlike FePIPG, washing FePSG and FeP-$SiSO_3^-$ in a Soxhlet extractor did not introduce any changes in these catalysts EPR spectra.

3.5. FeP-catalyzed epoxidation of (Z)-cyclooctene by PhIO in heterogeneous systems

Initial studies compared the catalytic activity of washed and unwashed Fe(TDCPP)IPG and Fe[M(4-*N*-MePy)TDCPP]IPG to see if there were differences in their catalytic activities. Table 2 shows that washing FePIPG in the Soxhlet extractor leads to better catalysts. Based on the catalyst characterization studies described above, unwashed Fe[M(4-*N*-MePy)

Table 2
Comparison of the catalytic activity of washed and unwashed FePIPG in the epoxidation of (*Z*)-cyclooctene by PhIO
Reaction conditions: Argon atmosphere, $T = 25$°C, magnetic stirring, $t = 1$ h, PhIO/FeP molar ratio = 100:1, 4.0×10^{-6} mol FeP/g IPG, 9.3×10^{-5} mol Im/g IPG, Im/FeP molar ratio = 20, [FeP] = 6.2×10^{-5} mol l^{-1}, (*Z*)-cyclooctene/FeP molar ratio = 5.8×10^{4}, solvent: DCE.

Catalyst	Washing	Cox (%)[a]
Fe(TDCPP)IPG	no	44
	yes	60
Fe[M(4-*N*-MePy)TDCPP]IPG	no	47
	yes	62

[a] *Cis*-epoxycyclooctane (Cox) yield based on PhIO.

TDCPP]IPG contains much more bis-imidazole $Fe^{III}P$ species than the washed catalyst. So, unwashed FePIPG gives rise to lower *cis*-epoxycyclooctane yields since FeP bis-ligation to IPG leads to a competition between PhIO and imidazole for the sixth coordination position in the FeP, making the formation of the $Fe^{IV}(O)P^{\cdot+}$ active species more difficult. Conversely, washed FePIPG catalysts lead to better results because they contain a smaller proportion of FeP bis-coordinated to the support.

Besides leading to lower yields, another problem was encountered with unwashed FePIPGs: FeP leaching from the support. The UV-Vis spectra of the reaction solutions where unwashed Fe(TDCPP)IPG and Fe[M(4-*N*-MePy)-TDCPP]IPG were used as catalysts revealed the presence of the characteristic FeP Soret band at $\lambda = 418$ and 420 nm, respectively. Such reaction solutions were isolated from the solid FePIPG catalysts by centrifugation and addition of more PhIO to these solutions gave further ~40% yield of *cis*-epoxycyclooctane. Consequently, the epoxide yields of 44% and 47% attained with unwashed Fe(TDCPP)IPG and Fe[M(4-*N*-MePy)TDCPP]IPG, respectively, are likely to be due to both heterogeneous and homogeneous catalysts. On the other hand, when washed Fe(TDCPP)IPG and Fe[M(4-*N*-MePy)TDCPP]IPG were used as catalysts, the UV-Vis spectra of the reaction solutions showed no evidence for any leached FeP and they were catalytically inactive when PhIO was added to them.

The catalytic activities of supported Fe[M(4-*N*-MePy)TDCPP]$^{2+}$ and Fe[M(4-*N*-MePy)-TFPP]$^{2+}$ were compared with those of supported Fe(TDCPP)$^{+}$ and Fe(TFPP)$^{+}$. The time-dependent build-up of *cis*-epoxycyclooctane was monitored for the (*Z*)-cyclooctene epoxidation

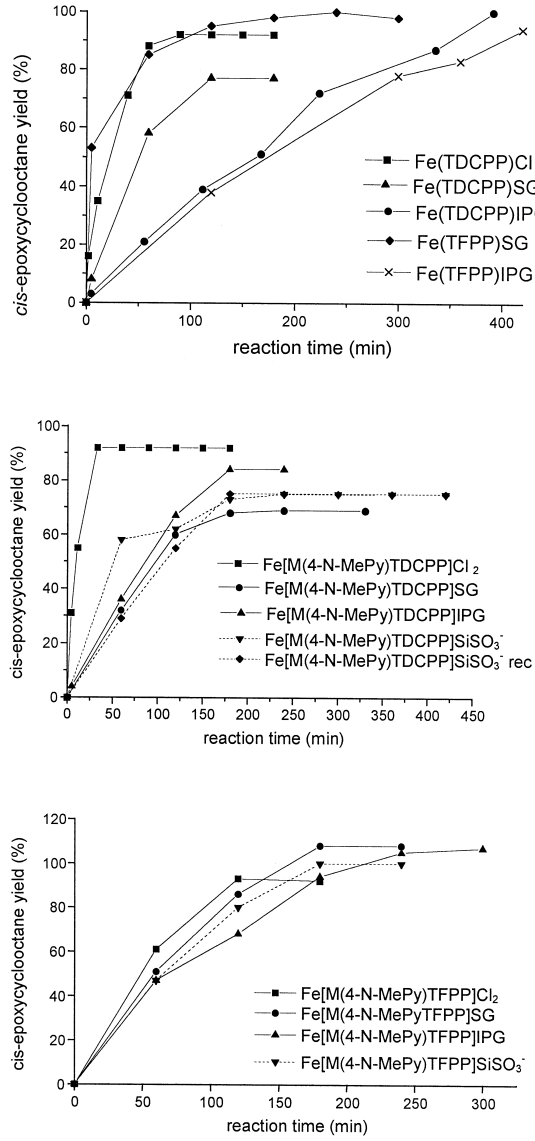

Fig. 10. Time-dependent build-up of *cis*-epoxycyclooctane in the epoxidation of (*Z*)-cyclooctene by PhIO catalyzed by various FePCl in homogenous and heterogenous systems.

Table 3
Catalytic activity of various supported FeP in the epoxidation of (*Z*)-cyclooctene by PhIO
Reaction conditions: Argon atmosphere, $T = 25$°C, magnetic stirring, PhIO/FeP molar ratio = 100:1, [FeP] = 3×10^{-4} mol l^{-1}, 4.0×10^{-6} mol FeP/g support.

FeP	Support	Cox (%)[a]	Reaction time (min)
Fe(TDCPP)	–	92	90
	SG	77	120
	IPG	100	420
Fe(TFPP)	–	80	60
	SG	94	180
	IPG	85	240
Fe[M(4-*N*-MePy)-TDCPP]	–	92	30
	SG	69	180
	IPG	84	180
	$SiSO_3^-$	75	180
	recycled $SiSO_3^-$	75	180
Fe[M(4-*N*-MePy)-TFPP]	–	92	120
	SG	100	180
	IPG	100	180
	$SiSO_3^-$	100	180

[a] *Cis*-epoxycyclooctane (Cox) yield based on PhIO.

by PhIO in all cases (Fig. 10; Table 3). Results obtained with homogeneous FePs are also presented for comparison.

In all the reactions, PhIO was totally consumed and the PhI yields were ca. 100%. No FeP leaching was observed in any of the reactions.

Results from Table 3 and Fig. 10 show that heterogeneous catalysts are slower than homogeneous analogues. It is likely that the active catalytic site in the supported FePs is considerably more polar than those of the FePs in DCE and this may disfavour the approach of the substrate (*Z*)-cyclooctene, which is apolar, and the diffusion of the product *cis*-epoxycyclooctane from the heterogeneous catalyst to bulk solution [15,17].

Immobilized $Fe(TFPP)^+$ and $Fe[M(4\text{-}N\text{-}MePy)TFPP]^{2+}$ lead to *cis*-epoxycyclooctane yields comparable to those obtained with the corresponding FePs in homogeneous solution. In the case of $Fe(TFPP)^+$, slightly better product yields are obtained because anchoring the catalyst prevents the formation of dimeric species $[Fe(TFPP)]_2O$. Similarly for $Fe[M(4\text{-}N\text{-}Me\text{-}Py)TFPP]^{2+}$, supporting the catalyst prevents FeP aggregation through $\pi-\pi$ interaction (Fig. 5), preventing catalyst deactivation.

Supported catalysts Fe(TDCPP)SG and Fe[M(4-*N*-MePy)TDCPP]SG lead to lower *cis*-epoxycyclooctane yields than their homogeneous counterparts. It is possible that this arises from FeP coordination to surface silanol groups, which will shift the iron out of the porphyrin plane and cause the chloro substituents located in the face opposite to support coordination to get closer. These effects will hinder the approach of the substrate to the active site of the catalyst.

It is important to emphasize that although Fe[M(4-*N*-MePy)TDCPP]IPG leads to lower *cis*-epoxycyclooctane yields than Fe(TDCPP)IPG (84% and 100%, respectively), the former leads to a shorter reaction time (180 and 420 min, respectively), compensating for its lower efficiency.

The new heterogeneous catalysts $Fe[M(4\text{-}N\text{-}MePy)TDCPP]SiSO_3^-$ and $Fe[M(4\text{-}N\text{-}MePy)TFPP]SiSO_3^-$, where the FePs bind to the support through electrostatic interaction, lead to yields similar to or better than the same FePs on SG or IPG. Recycling of the catalyst $Fe[M(4\text{-}N\text{-}MePy)TDCPP]SiSO_3^-$ shows that it maintains its catalytic activity in a second reaction (Table 3; Fig. 10). So, although the reactions catalyzed by supported FeP are slower than those carried out in homogeneous systems, the solid catalysts have the advantage of being easily recovered and re-used at the end of the reaction.

4. Conclusions

The new cationic FePs $Fe[M(4\text{-}N\text{-}MePy)TDCPP]Cl_2$ and $Fe[M(4\text{-}N\text{-}MePy)TFPP]Cl_2$ give comparable yields of *cis*-epoxycyclooctane to their apolar analogues Fe(TDCPP)Cl and Fe(TFPP)Cl in the epoxidation of (*Z*)-cyclooctene by PhIO. Binding Fe[M(4-*N*-MePy)TD-

CPP]Cl_2 and Fe[M(4-*N*-MePy)TFPP]Cl_2 to SG, IPG or $SiSO_3^-$ also leads to very efficient catalysts that can be easily recovered and re-used. Recycling of Fe[M(4-*N*-MePy)TDCPP]$SiSO_3^-$ shows that it maintains its catalytic activity in a second reaction.

The study of the interaction between the cationic FePs and the axial ligands imidazole and OH^- was very helpful to characterize the heterogeneous catalysts FePSG, FePIPG and $FePSiSO_3^-$ through UV-Vis and EPR spectroscopy. When supported on IPG, both cationic FePs bind to the support via Fe–imidazole coordination. Fe[M(4-*N*-MePy)TDCPP]IPG contains a mixture of low-spin bis-ligated $Fe^{III}P$ and high-spin mono-coordinated $Fe^{III}P$ species and Fe[M(4-*N*-MePy)TFPP]IPG contains high-spin mono-ligated $Fe^{III}P$. Both FePIPGs contain $Fe^{II}P$ species, whose presence was confirmed by EPR spectroscopy using NO as a paramagnetic probe. When anchored on SG, both cationic FePs coordinate to the support through Fe–O ligation and they are present as high-spin $Fe^{III}P$ species. The cationic catalysts on $SiSO_3^-$ are also high-spin $Fe^{III}P$ species and the FePs bind to the support via electrostatic interaction between the 4-*N*-methylpyridyl groups and the SO_3^- groups present on the support.

Further work in our laboratory will focus on the catalytic activity of the FePs in the oxidation of other hydrocarbons as well as on recycling experiments.

Acknowledgements

This work was supported by CAPES, CNPq and FAPESP. We are grateful to Dr. Eduardo J. Nassar for technical assistance and to Prof. Osvaldo Antonio Serra for helpful discussions.

References

[1] B. Meunier, Chem. Rev. 92 (1992) 1411.
[2] D. Mansuy, P. Battioni, J.P. Battioni, Eur. J. Biochem. 184 (1989) 267.
[3] D. Mansuy, Pure Appl. Chem. 59 (1987) 759.
[4] J.R. Lindsay-Smith, in: R.A. Sheldon (Ed.), Metalloporphyrins in Catalytic Oxidations, Marcel Dekker, New York, 1994, Chap. 11, p. 325.
[5] D. Mansuy, Coord. Chem. Rev. 125 (1993) 129.
[6] B.A. Arndtsen, R.G. Bergman, T.A. Mobley, T.H. Peterson, Acc. Chem. Res. 28 (1995) 154.
[7] J.T. Groves, T.E. Nemo, R.S. Myers, J. Am. Chem. Soc. 101 (1979) 1032.
[8] P.S. Traylor, D. Dolphin, T.G. Traylor, J. Chem. Soc., Chem. Commun. (1984) 279.
[9] C.K. Chang, F. Ebina, J. Chem. Soc., Chem. Commun. (1981) 778.
[10] T.G. Traylor, S. Tsuchiya, Inorg. Chem. 26 (1987) 1338.
[11] A.W. Van der Made, J.W.H. Smeets, R.J.M. Nolte, W. Drenth, J. Chem. Soc., Chem. Commun. (1983) 1204.
[12] E. Polo, R. Amadelli, V. Carassiti, A. Maldotti, Inorg. Chim. Acta Lett. 192 (1992) 1.
[13] O. Leal, D.L. Anderson, R.G. Bowman, F. Basolo, J. Burwell Jr., J. Am. Chem. Soc. 97 (1975) 5125.
[14] T. Tatsumi, M. Nakamura, H. Tominaga, Chem. Lett. (1989) 419.
[15] P.R. Cooke, J.R.L. Smith, J. Chem. Soc., Perkin Trans. 1 (1994) 1913.
[16] J.R. Lindsay-Smith, Y. Iamamoto, H.C. Sacco, Proc. 3rd Int. Symp. Supported Reagents and Catalysts in Chemistry, Universty of Limerick, Ireland, 8–11 July 1997, poster 38.
[17] C. Gilmartin, J.R.L. Smith, J. Chem. Soc., Perkin Trans. 2 (1995) 243.
[18] D.R. Leanord, J.R. Lindsay-Smith, J. Chem. Soc., Perkin Trans. 2 (1990) 1917.
[19] D.R. Leanord, J.R. Lindsay-Smith, J. Chem. Soc., Perkin Trans. 2 (1991) 25.
[20] B. Meunier, in: R.A. Sheldon (Ed.), Metalloporphyrins in Catalytic Oxidations, Marcel Dekker, New York, 1994, Chap. 5, p. 133.
[21] Y. Iamamoto, K.J. Ciuffi, H.C. Sacco, C.M.C. Prado, M. Moraes, O.R. Nascimento, J. Mol. Catal. 88 (1994) 167.
[22] Y. Iamamoto, H.C. Sacco, A.J.B. Melo, C.M.C. Prado, M.D. Assis, K.J. Ciuffi, L.S. Iwamoto, J. Braz. Chem. Soc. 6 (1995) 251.
[23] Y. Iamamoto, M.D. Assis, K.J. Ciuffi, H.C. Sacco, L.S. Iwamoto, A.J.B. Melo, O.R. Nascimento, C.M.C. Prado, J. Mol. Catal. A: Chem. 109 (1996) 189.
[24] Y. Iamamoto, H.C. Sacco, K.J. Ciuffi, L.S. Iwamoto, O.R. Nascimento, C.M.C. Prado, J. Mol. Catal. A: Chem. 116 (1997) 405.
[25] Y. Iamamoto, M.D. Assis, K.J. Ciuffi, C.M.C. Prado, B.Z. Prellwitz, M. Moraes, O.R. Nascimento, H.C. Sacco, J. Mol. Catal. A: Chem. 116 (1997) 365.
[26] Y. Iamamoto, M.D. Assis, K.J. Ciuffi, C.M.C. Prado, H.C. Sacco, A.P.J. Maestrin, A.J.B. Melo, O.R. Nascimento, O. Baffa, J. Mol. Catal. A: Chem. 117 (1997) 259.
[27] J.G. Sharefkin, H. Saltzmann, Org. Synth. 43 (1963) 62.
[28] A.D. Adler, F.R. Longo, F. Kampas, J. Kim, J. Inorg. Nucl. Chem. 32 (1970) 2443.
[29] A.D. Adler, F.R. Longo, W. Shergalis, J. Am. Chem. Soc. 86 (1964) 3145.
[30] A.D. Adler, F.R. Longo, J. Finarelli, J. Goldmacher, J. Org. Chem. 32 (1967) .

[31] C. Casas, B. Saint-Jalmes, C. Loup, C.J. Lacey, B. Meunier, J. Org. Chem. 58 (1993) 2913.
[32] O. Brigaud, Substitutions Aromatiques sur les meso-tetraarylporphyrines — synthese, étude structurale et catalytique de nouvelles métalloporphyrines polyhalogenées, PhD Thesis, Université de Paris, Paris, 1993.
[33] M.J. Nappa, C.A. Tolman, Inorg. Chem. 24 (1985) 4711.
[34] K. Kano, H. Minamizono, T. Kitae, S. Negi, J. Phys. Chem. A 101 (1997) 6118.
[35] K. Hatano, M.K. Safo, A.F. Walker, W.R. Scheidt, Inorg. Chem. 30 (1991) 1643.
[36] T.P. Wijesekera, D. Dolphin, in: R.A. Sheldon (Ed.), Metalloporphyrins in Catalytic Oxidations, Marcel Dekker, New York, 1994, Ch. 7, p. 193.
[37] E.B. Fleischer, D.A. Fine, Inorg. Chim. Acta 129 (1978) 267.
[38] L. Martin Neto, O.R. Nascimento, M. Tabak, I. Caracelli, Biochim. Biophys. Acta 956 (1988) 189.
[39] L. Martin Neto, O.R. Nascimento, M. Tabak, J. Inorg. Biochem. 40 (1990) 309.
[40] O.A. Serra, C.M.C. Prado-Manso, L.S. Iwamoto, Y. Iamamoto, Química Nova 22 (1999) 277.
[41] K. Hatano, M.K. Safo, A.F. Walker, W.R. Scheidt, Inorg. Chem. 30 (1991) 1643.
[42] H. Kobayashi, Y. Yanagawa, Osada, S. Minami, M. Shimizu, Bull. Chem. Soc. Jpn. 46 (1973) 1471.